

Scattering by a random set of parallel cylinders

D. Felbacq, G. Tayeb, and D. Maystre

Laboratoire d'Optique Electromagnétique, Unité de Recherche Associée au Centre National de la Recherche Scientifique No. 843, Faculté des Sciences et Techniques de St Jérôme (Case 262), 13397 Marseille Cedex 20, France

Received January 3, 1994; revised manuscript received April 20, 1994; accepted April 20, 1994

A theory of scattering by a finite number of cylinders of arbitrary cross section is presented. This theory is based on a self-consistent approach that identifies incident and scattered fields around each cylinder and then uses the notion of a scattering matrix in order to get a linear system of equations. Special attention is paid to the simplified case of a sparse distribution of small cylinders for low frequencies. Surprisingly, it is found that the classical rules of homogenization must be modified in that case. The phenomenon of enhanced backscattering of light is investigated from numerical data for a dense distribution of cylinders.

1. INTRODUCTION

The purpose of this paper is to present a theory of scattering by a finite set of parallel cylinders of arbitrary cross section arbitrarily distributed in a given region of space of cross section C . A rigorous self-consistent theory is used. A numerical implementation is achieved for various kinds of cylinder. Special attention is paid to the case of a distribution of cylinders having transversal dimensions that are small with respect to the wavelength of the light, for which case a simpler approximate theory can be used.

The possibilities of the homogenization process for the low-frequency range are investigated. From the numerical results it is shown that in general the classical rules of homogenization no longer hold for the case of low frequencies (when the size of C is much smaller than the wavelength) for a sparse distribution of cylinders. The correction to the classical rule is given and explained from theoretical considerations.

The phenomenon of enhanced backscattering¹ is investigated from numerical data for a dense and random distribution of cylinders. The strong influence of the shape of the cylinders on this phenomenon is studied numerically and explained from intuitive considerations.

2. PRESENTATION OF THE THEORY AND NOTATION

We consider in Fig. 1 a Cartesian coordinate system of axes xyz of origin O , the x - y plane being the cross-section plane of a set of N parallel cylinders of cross sections C_j and boundaries S_j ($j = 1, 2, \dots, N$) arbitrarily placed in region C . Each of these cylinders has a permittivity $\varepsilon_j = \nu_j^2$, C_j being included in a circle \mathcal{D}_j of center O_j and radius R_j . It is assumed that two arbitrary circles \mathcal{D}_j and \mathcal{D}_i have no intersection. Let us denote by \mathcal{D} (of radius R) the smallest circle of center O including C . In the air a homogeneous plane wave of wave vector \mathbf{k} ($k = |\mathbf{k}| = 2\pi/\lambda$) illuminates the cylinders with an angle of incidence α with respect to the x axis. For simplicity the theory will be described for an s -polarized field incident upon metallic or dielectric (non-magnetic) cylinders, with the electric field parallel to the

z axis, but generalization to p polarization and to magnetic or perfectly conducting materials does not present a problem. With use of a time dependence in $\exp(-i\omega t)$, the incident electric field is given by

$$\mathbf{E}^i = E^i \mathbf{u}_z = \exp[-ik(x \cos \alpha + y \sin \alpha)] \mathbf{u}_z. \quad (1)$$

The scattered field E^S is defined at any point in space as the difference between the total and the incident fields E and E^i (we define the scattered field everywhere for theoretical purposes, although its physical interpretation is not clear inside the cylinders):

$$E^S = E - E^i. \quad (2)$$

3. RIGOROUS THEORY

The total electric field satisfies, in the sense of distributions, the Helmholtz equation

$$\nabla^2 E + \tilde{k}^2(M)E = 0, \quad (3)$$

with

$$\tilde{k}^2(M) = k^2 \tilde{\varepsilon}(M) = \begin{cases} k^2 \varepsilon_j & \text{if } M \in C_j \ (j = 1, 2, \dots, N), \\ k^2 & \text{if } M \notin C_j \ (j = 1, 2, \dots, N), \end{cases} \quad (4)$$

M being an arbitrary point in space of coordinates (x, y) .

This Helmholtz equation may be rewritten in the form

$$\nabla^2 E + k^2 E = [k^2 - \tilde{k}^2(M)]E, \quad (5)$$

and, bearing in mind that the incident field satisfies the homogeneous Helmholtz equation

$$\nabla^2 E^i + k^2 E^i = 0, \quad (6)$$

we deduce by subtracting Eq. (6) from Eq. (5) that the scattered field satisfies

$$\nabla^2 E^S + k^2 E^S = [k^2 - \tilde{k}^2(M)]E, \quad (7)$$

which enables us to express the scattered field at any point P of space outside the cylinders, using Green's theorem:

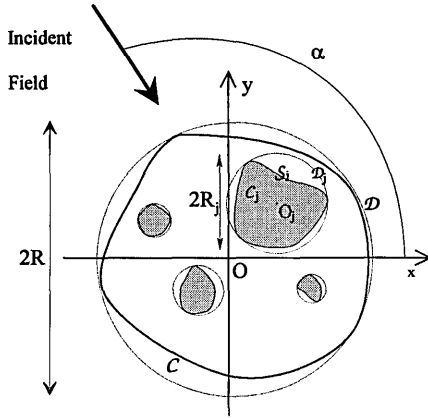


Fig. 1. General description of the problem and notation. See text for details.

$$E^S(P) = -\frac{i}{4} k^2 \iint H_0^{(1)}(kPM)[1 - \tilde{\epsilon}(M)]E(M)dxdy. \quad (8)$$

The integral on the right-hand side of Eq. (8) can be restricted to the set of cylinders C_j since $k^2 - \tilde{\epsilon}^2(M)$ vanishes outside the cylinders. This allows us to write the scattered field in the form of a sum of integrals on the cylinders:

$$E^S(P) = \sum_{j=1,2,\dots,N} \frac{ik^2(\epsilon_j - 1)}{4} \iint_{C_j} H_0^{(1)}(kPM)E(M)dxdy. \quad (9)$$

By definition, the j th term of the summation will be called the field scattered by the j th cylinder and denoted by E_j^S ; thus

$$E^S = \sum_{j=1,2,\dots,N} E_j^S, \quad (10)$$

with

$$E_j^S(P) = \frac{ik^2(\epsilon_j - 1)}{4} \iint_{C_j} H_0^{(1)}(kPM)E(M)dxdy. \quad (11)$$

In order to express E_j^S in a simpler form, let us consider in Fig. 2 the system of polar coordinates linked to the j th cylinder, with origin O_j . In this system point P is described by its polar angle $\theta_j(P)$ and its distance $r_j(P)$ to O_j . Using Graf's formula² for the Hankel function, if $r_j(M) \leq r_j(P)$

$$H_0^{(1)}(kPM) = \sum_{m=-\infty}^{+\infty} \exp[-im\theta_j(M)] \times J_m[kr_j(M)]H_m^{(1)}[kr_j(P)]\exp[im\theta_j(P)], \quad (12)$$

Eq. (11) yields

$$\forall P \text{ such that } r_j(P) \geq R_j,$$

$$E_j^S(P) = \sum_{m=-\infty}^{+\infty} b_{j,m}H_m^{(1)}[kr_j(P)]\exp[im\theta_j(P)], \quad (13)$$

with

$$b_{j,m} = \frac{ik^2(\epsilon_j - 1)}{4} \iint_{C_j} \exp[-im\theta_j(M)] \times J_m[kr_j(M)]E(M)dxdy. \quad (14)$$

Finally, insertion of the expression of E_j^S provided by Eq. (13) into Eq. (10) provides a modal expression of the total scattered field at any point outside the cylinders:

$\forall P$ outside the D_j ,

$$E^S(P) = \sum_{j=1,2,\dots,N} \sum_{m=-\infty}^{+\infty} b_{j,m}H_m^{(1)}[kr_j(P)]\exp[im\theta_j(P)]. \quad (15)$$

It is of fundamental importance to note that the existence of a modal expression of the field scattered by an arbitrary cylinder provided by Eq. (13) is quite general and extends to any kind of material (dielectric, metallic, magnetic, perfectly conducting, etc.), regardless of the incident polarization (p or s). However, this remark does not hold for Eq. (14). Since Eq. (13) is the basic equation of this theory and since Eq. (14) will not be used in what follows, it can be considered that what follows is quite general.

Equation (15) expresses the scattered field from the polar coordinates of P in the N coordinate systems linked to the cylinders. In order to obtain an expression of this field in a unique system of coordinates, for instance, the system linked to C_l , we express the right-hand side of Eq. (13) in the l th coordinate system by using Graf's formula and the notation of Fig. 2:

$$\begin{aligned} & \text{if } r_l(P) \leq r_l^j = O_lO_j, \\ & H_m^{(1)}[kr_j(P)]\exp[im\theta_j(P)] \\ &= \sum_{q=-\infty}^{+\infty} \exp[i(m - q)\theta_l^j]H_{q-m}^{(1)}(kr_l^j)J_q[kr_l(P)]\exp[iq\theta_l(P)] \end{aligned} \quad (16)$$

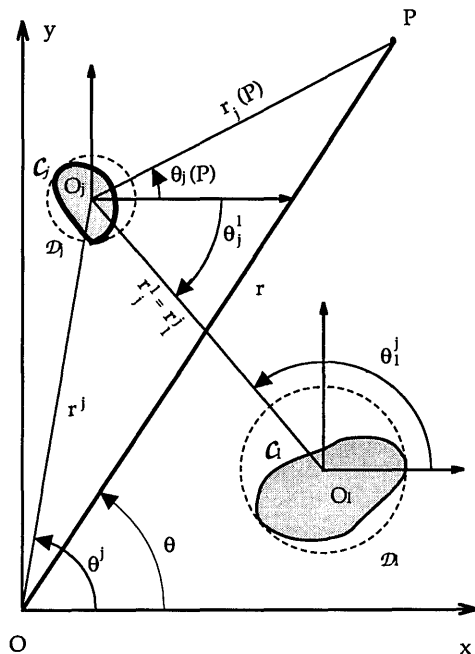


Fig. 2. Notation used for a change of the coordinate system of Bessel functions. The subscripts refer to the system of coordinates linked to a given cylinder. See text for details.

in such a way that Eq. (13) becomes

$$\forall P \text{ such that } r_l(P) \leq r_l^j - R_j, \\ E_j^s(P) = \sum_{m=-\infty}^{+\infty} b_{j,m} \sum_{q=-\infty}^{+\infty} \exp[i(m-q)\theta_l^j] \\ \times H_{q-m}^{(1)}(kr_l^j) J_q[kr_l(P)] \exp[iq\theta_l(P)]. \quad (17)$$

Similarly, the incident field given by Eq. (1) can be written in the form

$$E^i(P) = \exp[i\mathbf{k} \cdot \mathbf{OP}] = \exp[i\mathbf{k} \cdot (\mathbf{OO}_l + \mathbf{O}_l P)] \\ = \exp[-ikr^l \cos(\alpha - \theta^l)] \\ \times \exp[-ikr_l(P) \cos[\alpha - \theta_l(P)]], \quad (18)$$

and, using the classical formula

$$\exp(iz \cos u) = \sum_{n=-\infty}^{+\infty} (i)^n J_n(z) \exp(inu), \quad (19)$$

we can deduce from Eq. (18) that, at any point P in space,

$$E^i(P) = \exp[-ikr^l \cos(\alpha - \theta^l)] \sum_{n=-\infty, +\infty} (-i)^n \exp(-ina) \\ \times J_n[kr_l(P)] \exp[in\theta_l(P)]. \quad (20)$$

Finally, by adding the expression of the incident field given by Eq. (20), the expression of the field scattered by the cylinders C_j with $j \neq l$ given by Eq. (17) and the expression of the field scattered by C_l given by Eq. (13), we obtain a rigorous modal expansion of the field around C_l

$$\text{if } R_l \leq r_l(P) \leq \min_{j \neq l} (r_l^j - R_j), \\ E(P) = \sum_{m=-\infty, +\infty} a_{l,m} J_m[kr_l(P)] \exp[im\theta_l(P)] \\ + \sum_{m=-\infty, +\infty} b_{l,m} H_m^{(1)}[kr_l(P)] \exp[im\theta_l(P)], \quad (21)$$

with

$$a_{l,m} = (-i)^m \exp[-ikr^l \cos(\alpha - \theta^l) - im\alpha] \\ + \sum_{j \neq l} \sum_{q=-\infty, +\infty} b_{j,q} \exp[i(q-m)\theta_l^j] H_{m-q}^{(1)}(kr_l^j). \quad (22)$$

Denoting by $\hat{\mathbf{a}}_l$ and $\hat{\mathbf{b}}_l$ the infinite column matrix of components $a_{l,m}$ and $b_{l,m}$, we may write Eq. (22) in the matrix form

$$\hat{\mathbf{a}}_l = \mathbf{Q}_l + \sum_{j \neq l} \mathbf{T}_{l,j} \hat{\mathbf{b}}_j, \quad (23)$$

with \mathbf{Q}_l the column matrix of m th element $Q_{l,m}$ given by

$$Q_{l,m} = (-i)^m \exp[-ikr^l \cos(\alpha - \theta^l) - im\alpha] \quad (24)$$

and $\mathbf{T}_{l,j}$ a square matrix of the (m, q) th element $T_{l,j,m,q}$ given by

$$T_{l,j,m,q} = \exp[i(q-m)\theta_l^j] H_{m-q}^{(1)}(kr_l^j). \quad (25)$$

Equation (21) states a well-known result, summarized in Fig. 3: the field around C_j can be represented by a Fourier-Bessel modal expansion in the dashed annulus

located between \mathcal{D}_j and the circle of center O_j passing through the closest point of the other cylinders.³ The authors of Ref. 3 have used this property to solve the problem of scattering by a grating of circular cylinders under some conditions. It will be shown further that our method is more general. It is worth noting that the same kind of formalism has been used by other authors in the special case of circular cylinders.⁴⁻⁷ The concept of the scattering matrix will allow us to generalize it to arbitrary-shaped cylinders.

It is of fundamental importance to note that the two series in the right-hand side of Eq. (21) are quite different from a physical point of view. The first one, the coefficients of which are given by Eq. (22), represents the locally incident field, viz., the sum of the actual incident field and the field generated by the other cylinders in the direction of the l th cylinder, thus acting as secondary incident fields for this cylinder. On the other hand, the second term is the field scattered by the l th cylinder. It is well known that the coefficients of the scattered field and those of the locally incident field are linked by a matrix relation depending on the parameters of the l th cylinder only,

$$\hat{\mathbf{b}}_l = \mathbf{S}_l \hat{\mathbf{a}}_l, \quad (26)$$

where \mathbf{S}_l is an infinite square matrix. It is noteworthy that this definition of the scattering matrix is not the usual one, since in general the field around the l th cylinder is separated into incoming and outgoing fields (with Hankel functions of the second and first kinds, respectively). A straightforward calculation shows that our \mathbf{S} matrix is linearly linked to the classical one.

Equations (23) and (26) allow us to eliminate the matrices $\hat{\mathbf{a}}_l$, and, after multiplying Eq. (23) by \mathbf{S}_l and then using Eq. (26) to express the left-hand side, we obtain

$$\hat{\mathbf{b}}_l - \sum_{j \neq l} \mathbf{S}_l \mathbf{T}_{l,j} \hat{\mathbf{b}}_j = \mathbf{S}_l \mathbf{Q}_l. \quad (27)$$

This linear system of equations may be written in the form

$$\begin{bmatrix} \mathbf{I} & -\mathbf{S}_1 \mathbf{T}_{1,2} & -\mathbf{S}_1 \mathbf{T}_{1,3} & \dots & \dots \\ -\mathbf{S}_2 \mathbf{T}_{2,1} & \mathbf{I} & -\mathbf{S}_2 \mathbf{T}_{2,3} & \dots & \dots \\ -\mathbf{S}_3 \mathbf{T}_{3,1} & -\mathbf{S}_3 \mathbf{T}_{3,2} & \mathbf{I} & \dots & \dots \\ \dots & \dots & \dots & \dots & \dots \\ \dots & \dots & \dots & \dots & \dots \end{bmatrix} \begin{bmatrix} \hat{\mathbf{b}}_1 \\ \hat{\mathbf{b}}_2 \\ \hat{\mathbf{b}}_3 \\ \dots \\ \dots \end{bmatrix} = \begin{bmatrix} \mathbf{S}_1 \mathbf{Q}_1 \\ \mathbf{S}_2 \mathbf{Q}_2 \\ \mathbf{S}_3 \mathbf{Q}_3 \\ \dots \\ \dots \end{bmatrix}, \quad (28)$$

which is a linear system of equations, \mathbf{I} being the infinite unit matrix. If the square and column submatrices \mathbf{S}_l ,

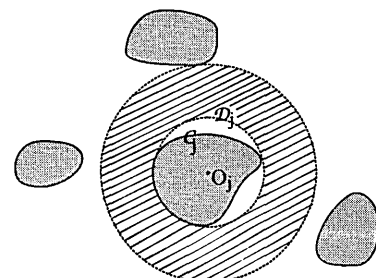


Fig. 3. Domain of validity of the Fourier-Bessel expansion of the total field around one cylinder.

$\mathbf{T}_{l,j}$, and $\hat{\mathbf{b}}_l$ are truncated in order to keep the indices m and q between $-M$ and $+M$ in Eqs. (21) and (22), the final size of the system to be inverted is $N(2M + 1)$.

Finally, let us express the scattered field outside \mathcal{D} (thus at infinity) from the column matrices $\hat{\mathbf{b}}_l$. With this aim, let us consider the expression of the scattered field outside the cylinders, given by Eq. (15). In order to express this scattered field in the system of coordinates xyz , we once more use Graf's formula:

if $r \geq r^j$,

$$H_m^{(1)}[kr_j(P)]\exp[im\theta_j(P)] = \sum_{q=-\infty,+\infty} \exp[i(m-q)\theta^j] \times J_{q-m}(kr^j)H_q^{(1)}(kr)\exp(iq\theta), \quad (29)$$

where r and θ are the polar coordinates of point P of space in the xy system.

With use of Eq. (29), Eq. (15) becomes, outside \mathcal{D} ,

$$E^S(P) = \sum_{q=-\infty,+\infty} b_q H_q^{(1)}(kr)\exp(iq\theta), \quad (30)$$

with

$$b_q = \sum_{j=1,N} \sum_{m=-\infty}^{+\infty} b_{j,m} \exp[i(m-q)\theta^j] J_{q-m}(kr^j). \quad (31)$$

At infinity the field can be expressed in a simpler way by use of the asymptotic form of the Hankel function²:

$$H_q^{(1)}(kr) \approx \sqrt{\frac{2}{\pi kr}} \exp\left[i\left(kr - q\frac{\pi}{2} - \frac{\pi}{4}\right)\right], \quad (32)$$

and Eq. (30) yields

$$E^S(P) \approx g(\theta) \frac{\exp(ikr)}{\sqrt{r}}, \quad (33)$$

with

$$g(\theta) = \sqrt{\frac{2}{\pi k}} \exp\left(-i\frac{\pi}{4}\right) \times \sum_{q=-\infty,+\infty} b_q \exp\left(-iq\frac{\pi}{2}\right) \exp(iq\theta). \quad (34)$$

The intensity at infinity (or the bistatic differential cross section) is defined by

$$D(\theta) = 2\pi |g(\theta)|^2; \quad (35)$$

and for lossless cylinders the energy balance criterion is written as

$$\int_0^{2\pi} |g(\theta)|^2 d\theta + 2\sqrt{\lambda} \operatorname{Re} \left[\exp\left(i\frac{\pi}{4}\right) g(\alpha + \pi) \right] = 0. \quad (36)$$

We obtain Eq. (36), the so-called optical theorem, by writing that the flux of the total field on a circle of center O and infinite in radius is equal to zero, since there is no loss of energy.⁸

4. SIMPLIFIED METHOD FOR LOW FREQUENCIES

A. Introduction

When the wavelength is large with respect to the size of each cylinder, important simplifications can be introduced into the rigorous theory that lead to a strong reduction of the size of the linear system to be inverted. Indeed, it will be shown that, under these conditions and for s polarization, the field scattered by each cylinder becomes isotropic, in such a way that the right-hand side of Eq. (13) reduces to the first term of the series.

Furthermore, if the size of the set of cylinders is small compared with the wavelength, the total field scattered by the cylinders is isotropic, as well. Hence it seems worthwhile to find an equivalence between this set of cylinders and a single homogeneous cylinder. This property will be used in Subsection 5.C below in order to define a homogenization process.

B. Preliminary Result: Scattering from a Subset of Cylinders in the Low-Frequency Domain

It is assumed that there exists a region $C' \subset C$ whose size is much smaller than the wavelength λ , containing N' cylinders ($1 \leq N' \leq N$). It is assumed that C' is included in a circle \mathcal{D}' of center O' and radius R' that contains the N' cylinders and nothing else (Fig. 4).

According to Eq. (8), the field $E^{S'}(P)$ scattered by the N' cylinders can be expressed in the form

$$E^{S'}(P) = -\frac{ik^2}{4} \iint_{C'} H_0^{(1)}(kPM)[1 - \tilde{\epsilon}(M)]E(M)dx dy. \quad (37)$$

In order to show that the scattered field becomes isotropic when kR' tends to zero, we consider a point P located at a distance $PO' \gg R'$. Noting (Fig. 4) that

$$PM = PO' + q(P, M),$$

with $|q(P, M)| < R'$, we deduce that in Eq. (37) the Hankel function can be expressed in the form

$$H_0^{(1)}(kPM) = H_0^{(1)}[kPO' + kq(P, M)] \approx H_0^{(1)}(kPO') - kq(P, M)H_1^{(1)}(kPO'). \quad (38)$$

Thus Eq. (37) takes the form

$$E^{S'}(P) = -\frac{i}{4} k^2 (I_1 + I_2), \quad (39)$$

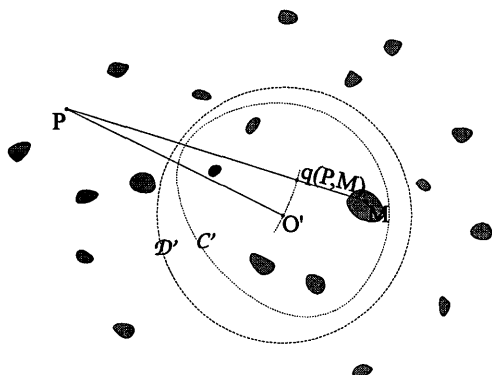


Fig. 4. Simplified method for low frequencies.

with

$$I_1 = H_0^{(1)}(kPO') \iint_{C'} [1 - \tilde{\epsilon}(M)] E(M) dx dy, \tag{39'}$$

$$I_2 = -H_1^{(1)}(kPO') \iint_{C'} kq(P, M) [1 - \tilde{\epsilon}(M)] E(M) dx dy. \tag{39''}$$

The integral on the right-hand side of Eq. (39') is independent of P and is *a priori* different from zero. Its calculation is straightforward as soon as the total field $E(M)$ is known inside C' . Assuming that the total field remains square integrable, this integral tends to a finite value when k tends to zero. In the same way, the integral on the right-hand side of Eq. (39'') remains finite as k tends to zero, and we deduce, taking into account the behavior of the Hankel function when the argument tends to zero, that the limit of the scattered field, when k tends to zero, is given by

$$\forall P, \text{ if } k \rightarrow 0,$$

$$E^{S'}(P) \approx Ak^2 \log(k) + k^2 B(P), \tag{40}$$

where A , coming from Eq. (39'), is a constant.

Thus, when k tends to zero, the leading term is the first one. It is noteworthy that, because $E^{S'}(P)$ tends to zero with k , the limit of $E(M)$ reduces to the local incident field, viz., the sum of the incident plane wave and the field scattered by the cylinders located outside C' .

This proof does not hold for p polarization, because basic equation (3) must be replaced by a more complicated one:

$$\nabla^2 H + \tilde{k}^2 H = [dH/dn] \delta_S, \tag{41}$$

where H is the z component of the magnetic field and $[dH/dn] \delta_S$ the symbol of a distribution⁹ having a support localized on $S = \cup_j S_j$, the set of boundaries of the cylinders, and defined by

$$\langle [dH/dn] \delta_S, \varphi \rangle = \int_S [dH/dn](M) \varphi(M) dl, \tag{42}$$

φ being an infinitely differentiable function of two variables with compact support,⁹ dl a differential element of the curvilinear abscissa on S , and $[dH/dn]$ the jump of the normal derivative of H on S .

From Eq. (41) it can be deduced that

$$\nabla^2 H^S + k^2 H^S = [k^2 - \tilde{k}^2(M)] H + [dH/dn] \delta_S, \tag{43}$$

which allows us to express the scattered field H^S at any point P outside the cylinders:

$$H^S(P) = -\frac{i}{4} k^2 \iint_C H_0^{(1)}(kPM) [1 - \tilde{\epsilon}(M)] \times H(M) dx dy - \frac{i}{4} \int_S H_0^{(1)}(kPM) \left[\frac{dH}{dn} \right] (M) dl. \tag{44}$$

Now let us use Eq. (44) for the subset C' of C , with boundary S' . Using relation (38), we obtain the field $H^{S'}(P)$ scattered by this subset by

$$H^{S'}(P) = -\frac{i}{4} k^2 H_0^{(1)}(kPO') \iint_{C'} [1 - \tilde{\epsilon}(M)] H(M) dx dy - \frac{i}{4} H_0^{(1)}(kPO') \int_{S'} \left[\frac{dH}{dn} \right] dl + \frac{i}{4} k^3 H_1^{(1)}(kPO') \iint_{C'} q(P, M) \times [1 - \tilde{\epsilon}(M)] H(M) dx dy + \frac{i}{4} k H_1^{(1)}(kPO') \int_{S'} q(P, M) \left[\frac{dH}{dn} \right] dl. \tag{45}$$

This expression can be simplified if we note that

$$\iint_{C'} k^2 [1 - \tilde{\epsilon}(M)] H(M) dx dy + \int_{S'} \left[\frac{dH}{dn} \right] dl = 0. \tag{46}$$

Indeed, inside each cylinder C_j ($j \in \{1, \dots, N'\}$), the magnetic field satisfies, in the sense of the functions,

$$\text{div}(\text{grad } H) + k^2 \epsilon_j H = 0, \tag{47}$$

and, by integrating on C_j and using the theorem of divergence, we obtain

$$\int_{S_j} \frac{dH}{dn_-} dl + k^2 \iint_{C_j} \epsilon_j H dx dy = 0, \tag{48}$$

the normal derivative being taken inside the cylinder C_j , with normal \mathbf{n} oriented toward the exterior.

Noting that

$$\frac{dH}{dn_-} = \epsilon_j \frac{dH}{dn_+},$$

we see from Eq. (48) that

$$\int_{S_j} \frac{dH}{dn_+} dl + k^2 \iint_{C_j} H dx dy = 0, \tag{49}$$

and thus, by subtracting Eq. (48) from Eq. (49), that

$$\int_{S_j} \left[\frac{dH}{dn} (M) \right] dl + k^2 \iint_{C_j} (1 - \epsilon_j) H(M) dx dy = 0. \tag{50}$$

We obtain Eq. (46) by summing Eq. (50) over each value of $j \in \{1, \dots, N'\}$.

Finally, the two remaining integrals in Eq. (45) can be simplified when $PO' \gg R'$, by use of an approximate value of $q(P, M)$.

Recalling that $q(P, M) = PM - PO'$ and $O'P \gg O'M$, we obtain

$$q \approx -\frac{O'P \cdot O'M}{O'P} \tag{51}$$

in such a way that Eq. (45) yields

$$H^{S'} \approx -\frac{i}{4} \frac{O'P}{O'P} \cdot \mathbf{V} H_1^{(1)}(kO'P), \tag{52}$$

where \mathbf{V} is a vector independent of P :

$$\mathbf{V} = \iint_{C'} k^3 [1 - \tilde{\epsilon}(M)] H(M) \mathbf{O}' M dx dy + \int_{S'} k \left[\frac{dH}{dn} \right] \mathbf{O}' M dl. \tag{53}$$

Assuming that H and dH/dn remain square integrable as k tends to zero, it can be shown that the first integral in Eq. (53) behaves like k^3 and the second one like k^2 (because dH/dn , like dH^i/dn , behaves like k).

Expressing the scattered field $H^{S'}(P)$ as in Eq. (30), we find that

$$H^{S'}(P) = \sum_{m=-\infty}^{+\infty} b'_m H_m^{(1)}(kr') \exp(im\theta'), \quad (54)$$

and it can be deduced from relation (52) that this expansion reduces to the terms $m = \pm 1$, with

$$b'_{\pm 1} = \mp \frac{i}{8} (V_x \mp iV_y). \quad (55)$$

C. Numerical Implementation of the Simplified Method

Here we restrict our study to s -polarized light, but this simplified method could be extended to p polarization, as well.

We use the results of Subsection 4.B, with a subset C' reduced to each of the cylinders C_j , which requires that the size of each cylinder be small with respect to the wavelength.

Under these conditions the field scattered by each cylinder at infinity is isotropic, and Eq. (13) becomes,

$$\text{if } r_j(P) \gg R_j, \quad E_j^S(P) \approx b_{j,0} H_0^{(1)}[kr_j(P)]. \quad (13')$$

In the same way, the expression of the incident field on the cylinder C_j can be restricted to the zeroth-order term, and Eq. (20) becomes, in the vicinity of C_l ,

$$E^i(P) \approx \exp[-ikr' \cos(\alpha - \theta^l)]. \quad (20')$$

Finally, the field scattered by an arbitrary cylinder C_j must be considered around C_l ($l \neq j$) as a local incident field. With our hypothesis, the expression of this field becomes, in the vicinity of C_l ,

$$E_j^S(P) \approx b_{j,0} H_0^{(1)}(kr_j^l).$$

Under these conditions, the total field around C_l can be written as

$$E(P) = \exp[-ikr^l \cos(\alpha - \theta^l)] + \sum_{j \neq l} b_{j,0} H_0^{(1)}(kr_j^l) + b_{l,0} H_0^{(1)}[kr_l(P)] \quad (21')$$

in such a way that Eq. (23) becomes a scalar equation:

$$a_{l,0} = Q_{l,0} + \sum_{j \neq l} T_{l,j,0,0} b_{j,0}, \quad (23')$$

and because Eq. (26) becomes scalar as well,

$$b_{l,0} = S_{l,0,0} a_{l,0}. \quad (26')$$

The linear system of equations [Eq. (27)] can be written in the form

$$b_{l,0} - \sum_{j \neq l} S_{l,0,0} T_{l,j,0,0} b_{j,0} = S_{l,0,0} Q_{l,0}. \quad (27')$$

Finally, in Eq. (28) all the square and column matrices are replaced by scalar numbers. Thus we get a system of N equations with N unknowns $b_{l,0}$:

$$\begin{bmatrix} 1 & -S_{1,0,0} H_0^{(1)}(kr_1^2) & -S_{1,0,0} H_0^{(1)}(kr_1^3) & \dots \\ -S_{2,0,0} H_0^{(1)}(kr_2^1) & 1 & \dots & \dots \\ \dots & \dots & \dots & \dots \\ \dots & \dots & \dots & \dots \end{bmatrix} \begin{bmatrix} b_{1,0} \\ b_{2,0} \\ \dots \\ \dots \end{bmatrix} = \begin{bmatrix} S_{1,0,0} \exp[-ikr^1 \cos(\alpha - \theta^1)] \\ S_{2,0,0} \exp[-ikr^2 \cos(\alpha - \theta^2)] \\ \dots \\ \dots \end{bmatrix}. \quad (28')$$

This system may be symmetrized by division of the j th line by $S_{j,0,0}$.

The expression of the scattered field outside C is given by Eqs. (30) and (31) being replaced by

$$b_m = \sum_{j=1,N} b_{j,0} \exp(-im\theta^j) J_m(kr^j). \quad (31')$$

Moreover, when the size of C is much smaller than λ , $kr^j \ll 1$, and thus the total scattered field reduces to the zeroth term:

$$b_0 = \sum_{j=1,N} b_{j,0}. \quad (31'')$$

It turns out that the total scattered field is isotropic, a result already predicted in Subsection 4.B.

5. NUMERICAL APPLICATION

A. Tests of Validity

The use of our formalism needs a prior solution of the problem of scattering by a single cylinder. For circular cylinders the scattering matrices S_l of Eq. (26) are obtained from the classical method when the Fourier–Bessel expansions of the fields inside and outside the cylinder are matched on the surface.⁸ For arbitrary shapes a rigorous finite-element method on the boundary based on an integral equation¹⁰ has been implemented. Both methods provide very precise results (generally to within 10^{-3}). With use of the new formalism for many cylinders, we have implemented numerous classical tests of validity on the numerical results (convergence of the results when the number $2M + 1$ of terms in the Fourier–Bessel expansions increases, energy balance for lossless materials, reciprocity).

For example, Fig. 5(a) shows a scattering object made of seven perfectly conducting cylinders of various shapes. Figure 5(b) gives the intensity of the scattered field for an s -polarized incident field with incidence angle $\pi/2$ and wavelength $\lambda = 1$ mm. This scattered intensity was computed for three values of $2M + 1$, between $\theta = 0^\circ$ and $\theta = 180^\circ$ (the region $180^\circ < \theta < 360^\circ$ has been removed from the curve since the scattered intensity is very large for $\theta \approx 270^\circ$). A convergence is obtained above $M = 9$. For $M = 9$ and $M = 14$ the energy balance criterion is satisfied to within 10^{-4} . The computation time on an IBM RS/6000-560 computer with 30 MFlops was 25 s for $M = 9$.

From these tests it turns out that the precision remains nearly the same as for a single cylinder, but of course the computation time increases with the number of cylinders since the size of the linear system to be solved increases with this number.

We compared the results of our theory with those of other theories. Figure 6(b) shows the scattering diagram of a set of two identical dielectric circular cylinders [Fig. 6(a)] illuminated by an s -polarized light. This curve was computed successively with our method and the method of fictitious sources.¹¹ The two curves are

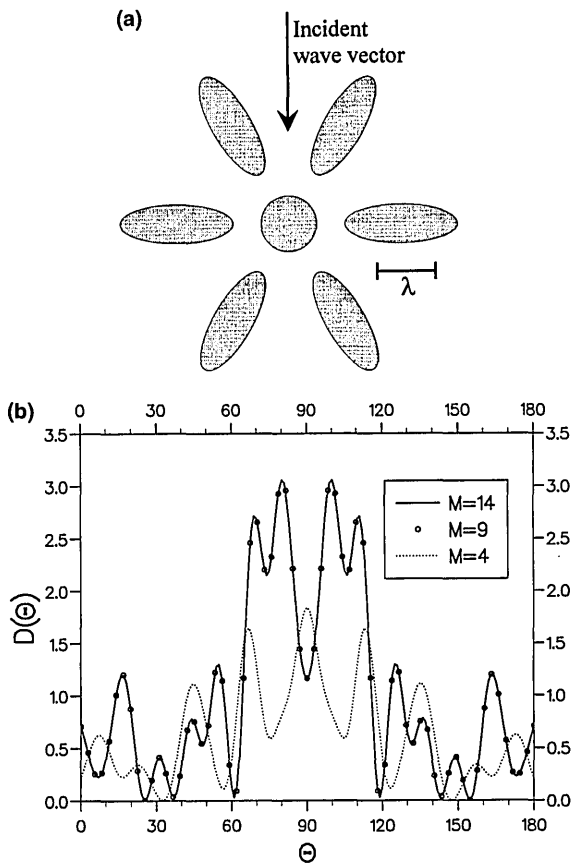


Fig. 5. Test of validity on a scattering object. (a) Scattering object: the central circular cylinder has diameter λ , and the ellipses have large and small axes, of 2λ and $2\lambda/3$, respectively. The centers of the circle and of one ellipse are separated by 3λ . (b) Convergence of the intensity radiated by the scatterer shown in (a).

identical, because the relative discrepancy is always less than 10^{-7} .

B. Phenomenon of Enhanced Backscattering

The phenomenon of enhanced backscattering by particles or by random rough surfaces has been investigated both theoretically and experimentally.¹²⁻¹⁸

In Ref. 18 Greffet studied diffraction by a set of square dielectric rods for *s* polarization. We performed calculations with similar data but replaced the square rods of side $\lambda/10$ with circular ones of diameter $\lambda/10$. Our results are shown in Fig. 7. Our curves are very similar to those of Greffet (Fig. 2 of Ref. 18), except for a scale factor that is due to the difference between the scattering objects and the wavelengths.

In the same paper,¹⁸ Greffet recalled previous results obtained by Maradudin *et al.*¹⁶ and conjectured that the enhanced backscattering phenomenon no longer holds for *p* polarization with a low index value. We now show that this prediction may be erroneous.

Figure 8(a) shows the intensity scattered by a set of 20 cylinders for *p* polarization. Obviously, a strong enhanced backscattering phenomenon is obtained, a fact that contradicts the conjecture of Greffet.¹⁸ Since this conjecture was deduced from numerical results obtained by Maradudin *et al.*,¹⁶ we tried to check the conclusion of

these authors, as well. In Ref. 16 the scattering object is a dielectric randomly rough surface with index 1.628. In order to simulate this kind of scattering object, we considered a set of 20 circular cylinders of index 1.5 placed on the same line, separated by random distances [Fig. 8(b)]. The peak at an angle of diffraction of 70° represents the specular direction of reflection by a mirror on the *x* axis, and the diffuse peak at $\sim 40^\circ$ is the direction of the first order that would be generated by a wire grating of groove spacing 3λ (average of the distance between two consecutive cylinders). Obviously, the peak of enhanced backscattering has disappeared, which confirms the conclusion of Maradudin *et al.*¹⁶ To explain this surprising difference between the two distributions of cylinders, we can notice that in Fig. 8(a) each cylinder is coupled with numerous other cylinders in the vicinity. On the other hand, in Fig. 8(b) each scatterer is coupled with two other scatterers placed in the vicinity, the other ones being masked in addition by a shadowing effect. The enhanced backscattering effect generated by the coupling between cylinders is therefore much greater in Fig. 8(a). This is all the more noticeable since the mean distance between two consecutive cylinders is equal to 3λ in Fig. 8(b), whereas the mean distance between two adjacent cylinders in Fig. 8(a) reaches almost 5λ .

Figure 9 shows that significant enhanced backscattering phenomena still appear for an index of 1.1 but disappear completely for an index of 1.05.

In conclusion, it emerges that the conditions for observing enhanced backscattering for dielectric diffracting objects are difficult to outline. They depend not only on the polarization and the indices but also on the geometric distribution and the size of the cylinders.

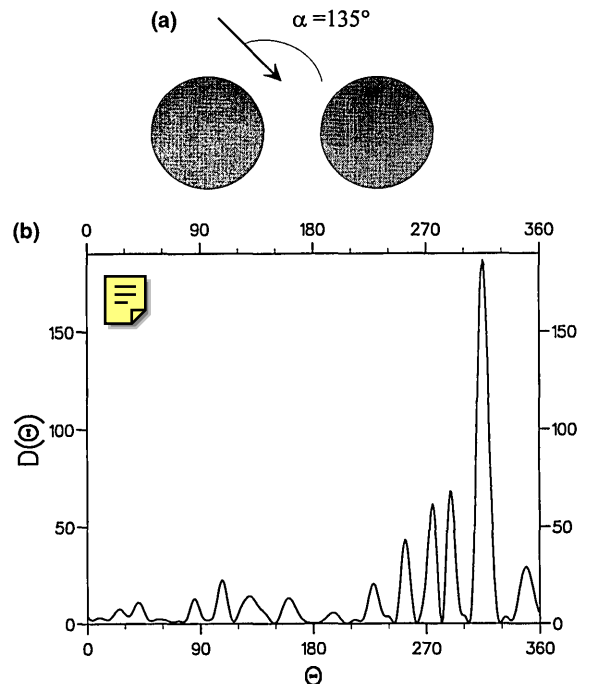


Fig. 6. Comparison with another theory. (a) Scattering object: two dielectric circular cylinders (index 1.5) with diameter 60 mm, distance between centers 90 mm, and *s*-polarized light. (b) Scattered intensity versus diffraction angle for a wavelength of 30 mm, incidence $\alpha = 135^\circ$, and *s*-polarized light.

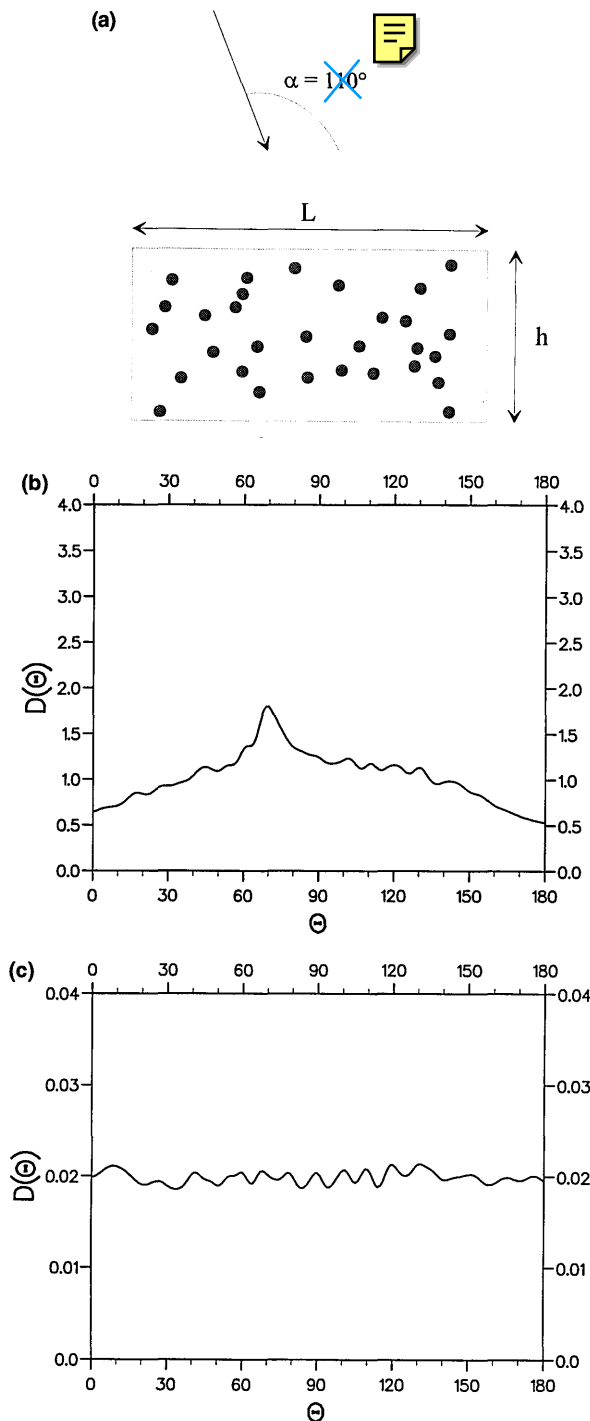


Fig. 7. Scattering by a set of cylinders. (a) 30 cylinders of diameter $\lambda/10$, randomly placed in a rectangular box; $L = 10\lambda$, $h = 5\lambda$, s polarization. (b), (c) Scattered intensity $D(\theta)$ corresponding to cylinders of indices $\nu = 4$ and $\nu = 1.5$, with wavelength $\lambda = 1$ mm. The results are averaged over 1000 realizations.

In Figs. 10–13 we show the influence on enhanced backscattering of the scattering diagram of a single diffracting cylinder.

Figure 10 gives the scattering cross section of a single perfectly conducting square cylinder with one side lying on the x axis; Fig. 11 shows the cross section of the same cylinder, but the cylinder is rotated by 45° around the z axis. The backscattered intensity is much greater in

Fig. 10 than in Fig. 11. As a consequence, it can be conjectured that the phenomenon of enhanced backscattering generated by a random set of cylinders similar to that of Fig. 11 should be stronger than when the cylinders are those of Fig. 10. Indeed, contrary to what happens for rods such as shown in Fig. 10, the origin of enhanced backscattering, i.e., the multiscattering phenomenon, is not challenged by a strong single scattering for rods such as shown in Fig. 11.

Figures 12 and 13 fully confirm the above prediction. Of course, this rule should not be considered a general one, at least so long as it has not been checked by numerous other calculations.

C. Homogenization Process for Low Frequencies

From Section 4 we know that for s polarization the total field scattered by the cylinders is isotropic, provided that the size of the set of cylinders is small compared with the wavelength. Hence it seems worthwhile to try to find an equivalence between such a set of cylinders and a single homogeneous cylinder. In other words, we will try to define the homogenization process. The laws of

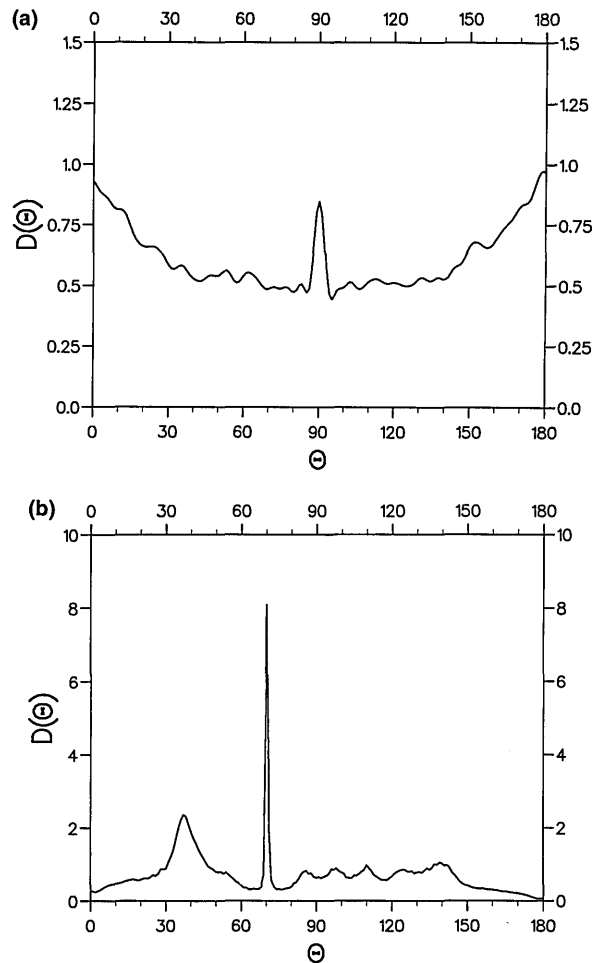


Fig. 8. Scattered intensity $D(\theta)$ produced by a set of 20 cylinders of diameter 1.2λ and p polarization. The results are averaged over 1000 realizations. Indices: $\nu = 1.5$, $\lambda = 1$ mm. (a) Cylinders randomly placed in a circular box of diameter $2R = 28\lambda$; angle of incidence, $\alpha = 90^\circ$. (b) Cylinders randomly placed on the x axis. The distance between the centers of two consecutive cylinders is a uniform random distribution between 1.2 and 4.8λ . Angle of incidence, $\alpha = 110^\circ$.

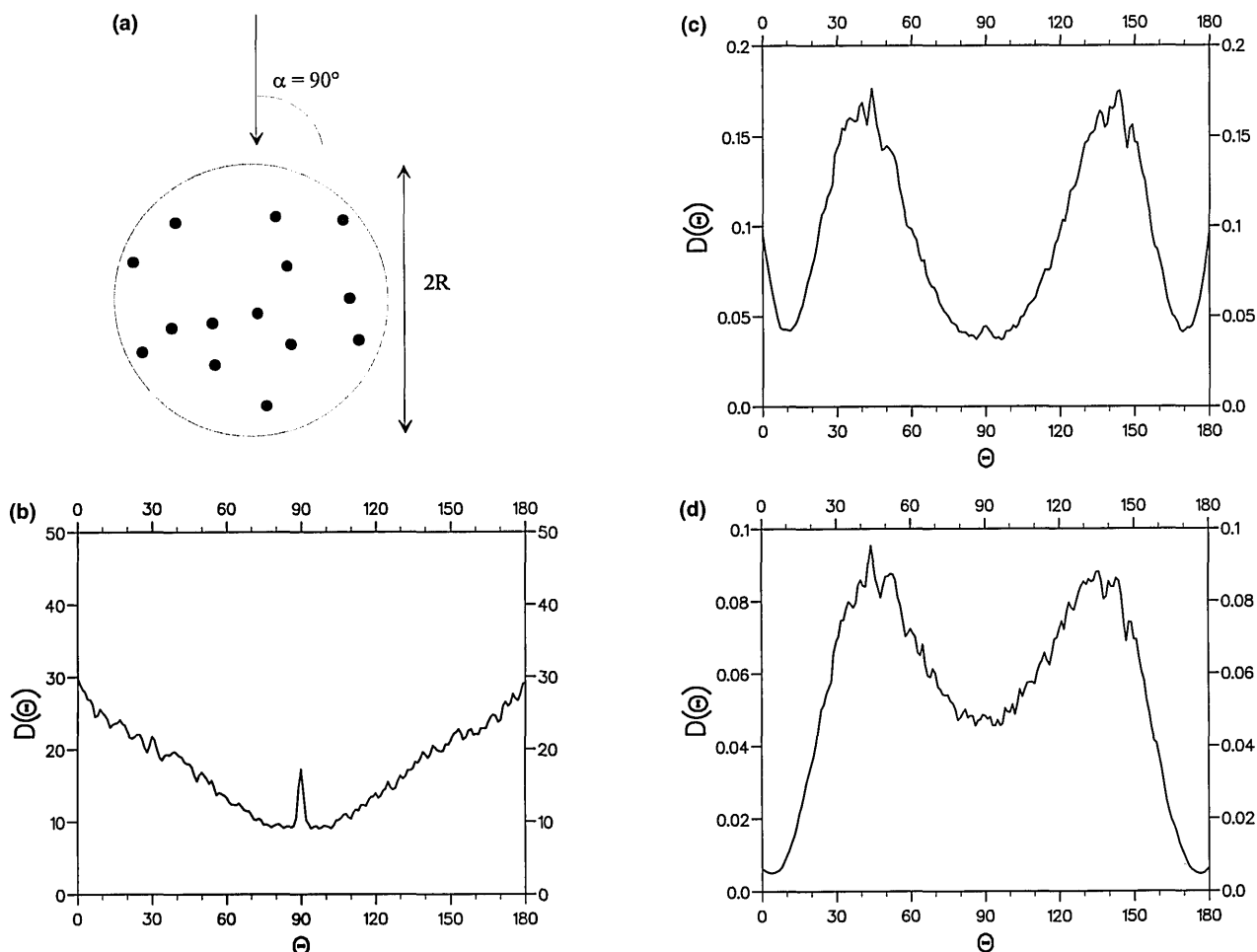


Fig. 9. Scattering by a set of 20 cylinders of diameter λ , randomly placed in a circular box of diameter $2R = 28\lambda$, for p polarization, $\alpha = 90^\circ$, and $\lambda = 30$ mm. The results are averaged over 1000 realizations. (a) Scheme of the cylinders; (b), (c), (d) scattered intensity $D(\theta)$ corresponding to cylinders of indices $\nu = 1.5$, $\nu = 1.1$, and $\nu = 1.05$, respectively.

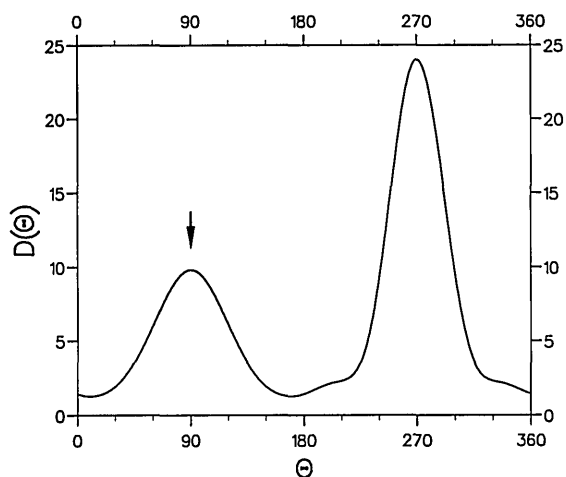


Fig. 10. Scattered intensity of a single perfectly conducting square cylinder of side 21 mm (one side lying on the x axis) illuminated for s polarization, $\alpha = 90^\circ$, and $\lambda = 30$ mm. The arrow indicates the backscattering direction.

homogenization are well known for the case in which the size of the set of particles is large with respect to the wavelength and for a high density of scatterers. We will show theoretically that these laws must be corrected at low frequencies in order for a boundary effect to be

taken into account. These theoretical predictions will be checked by numerical results.

We consider a set of N identical circular cylinders, with a circular cross section of radius ρ ($\forall j, R_j = \rho$) and a permittivity $\epsilon = \nu^2$. The cylinders are assumed to be randomly positioned in a domain C included in a circular

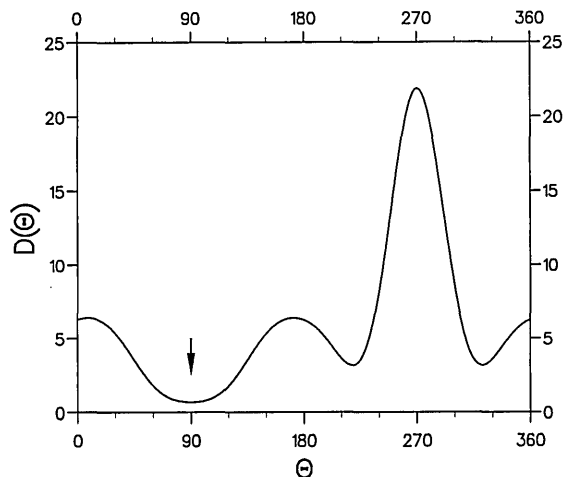


Fig. 11. Same as for Fig. 10 but with the square cylinder rotated 45° with respect to the z axis.

domain \mathcal{D} of radius R (see Fig. 1), with $R \ll \lambda$. The light is s polarized. From Section 4 we know that the scattered field outside \mathcal{D} is given by

$$E^S(P) = b_0 H_0^{(1)}(kr) = \left(\sum_{j=1,N} b_{j,0} \right) H_0^{(1)}(kr). \quad (56)$$

Our goal is to find the radius \tilde{R} and the permittivity $\tilde{\varepsilon} = \tilde{\nu}^2$ of an equivalent cylinder that gives the same diffracted field as the set of cylinders. In other words, the field scattered by this homogeneous single cylinder is written as

$$E^S(P) = \tilde{b}_0 H_0^{(1)}(kr), \quad (57)$$

and we seek \tilde{R} and $\tilde{\varepsilon}$ that realize $\tilde{b}_0 = b_0$.

Of course, the solution of this problem is not unique. In fact, there exists an infinity of homogeneous cylinders satisfying this requirement. Let us consider the simplest case, in which C and \mathcal{D} are identical. The classical rule of homogenization states that the radius of the equivalent cylinder is the same as that of \mathcal{D} and that its permittivity $\tilde{\varepsilon}$ is given by

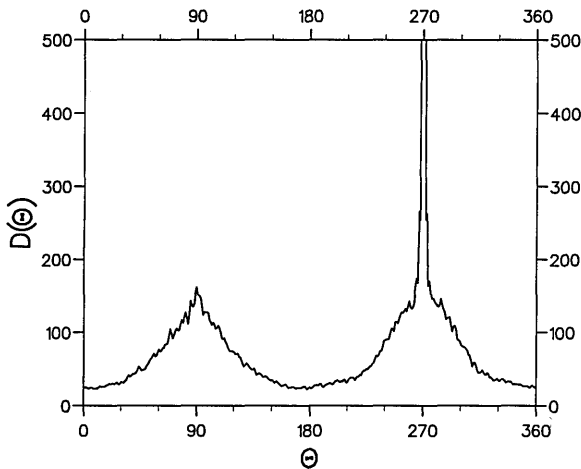


Fig. 12. Scattered intensity produced by a set of 20 square cylinders similar to the cylinder of Fig. 10 and randomly placed in a circular box of diameter $2R = 28\lambda$. The results are averaged over 1000 realizations.

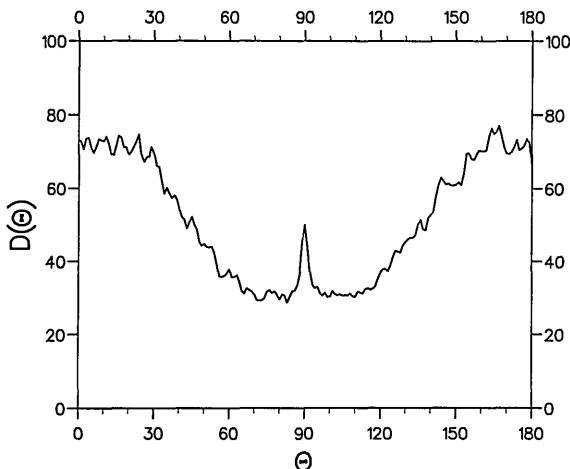


Fig. 13. Same as for Fig. 12 but with square cylinders similar to the cylinder of Fig. 11.

$$(\tilde{\varepsilon} - 1)R^2 = (\varepsilon - 1)N\rho^2. \quad (58)$$

It will be shown below that for low frequencies this rule must be corrected, for instance, by change of the actual radius, R , to a new one, \tilde{R} .

First, let us recall that for s polarization the amplitude \tilde{b}_0 scattered by a circular cylinder of radius \tilde{R} and permittivity $\tilde{\varepsilon}$, centered at the origin of coordinates and illuminated by a plane wave of unit amplitude, is given by

$$\tilde{b}_0 = \frac{J_1(k\tilde{R})J_0(k\tilde{\nu}\tilde{R}) - \tilde{\nu}J_0(k\tilde{R})J_1(k\tilde{\nu}\tilde{R})}{\tilde{\nu}H_0^{(1)}(k\tilde{R})J_1(k\tilde{\nu}\tilde{R}) - H_1^{(1)}(k\tilde{R})J_0(k\tilde{\nu}\tilde{R})}. \quad (59)$$

It is convenient to write this expression as

$$\tilde{b}_0 = \frac{1}{-1 + i\tilde{X}}, \quad (60)$$

where

$$\tilde{X} = \frac{\tilde{\nu}Y_0(k\tilde{R})J_1(k\tilde{\nu}\tilde{R}) - Y_1(k\tilde{R})J_0(k\tilde{\nu}\tilde{R})}{J_1(k\tilde{R})J_0(k\tilde{\nu}\tilde{R}) - \tilde{\nu}J_0(k\tilde{R})J_1(k\tilde{\nu}\tilde{R})}. \quad (61)$$

Assuming that $k\tilde{R} \ll 1$, Eq. (61) yields

$$\begin{aligned} \tilde{X} = & \frac{-4}{\pi(\tilde{\varepsilon} - 1)(k\tilde{R})^2} - \frac{2}{\pi} \log(k\tilde{R}) \\ & + \frac{1 - 4\gamma + 4 \log 2}{2\pi} - \frac{1}{\pi(\tilde{\varepsilon} - 1)} + O(k\tilde{R})^2, \end{aligned} \quad (62)$$

where γ is the Euler constant.

Now we consider a set of N identical cylinders. Starting from Eq. (27'), denoting by S the identical values of $S_{l,0,0}$ and noting that

$$Q_{l,0} = \exp[-ikr^l \cos(\alpha - \theta^l)] \approx 1,$$

we get

$$b_{l,0} - \sum_{j \neq l} S T_{l,j,0,0} b_{j,0} = S. \quad (63)$$

By adding the N equations ($l \in \{1, \dots, N\}$) and by separating $b_{l,0}$ into a mean value $\langle b_{l,0} \rangle$ and a deviation δ_l , we get

$$\begin{aligned} N\langle b_{l,0} \rangle - S\langle b_{l,0} \rangle \sum_{l=1,N} \sum_{j \neq l} T_{l,j,0,0} \\ - S \sum_{l=1,N} \sum_{j \neq l} \delta_j T_{l,j,0,0} = NS, \end{aligned}$$

and thus $\langle b_{l,0} \rangle$ can be expressed by

$$\langle b_{l,0} \rangle = S \frac{1 - D_1}{1 - D_2}, \quad (64)$$

with

$$\begin{aligned} D_1 &= \frac{1}{N} \sum_{l=1,N} \sum_{j \neq l} \delta_j T_{l,j,0,0}, \\ D_2 &= \frac{S}{N} \sum_{l=1,N} \sum_{j \neq l} T_{l,j,0,0}. \end{aligned}$$

It is noteworthy that D_1 and D_2 are corrections imposed by the coupling between the cylinders, $b_{l,0} = \langle b_{l,0} \rangle = S$ representing the limit value obtained by neglect of the

coupling (the local incident field being thus reduced to the incident plane wave).

With our assumption, i.e., a mean distance between cylinders much greater than the radius of these cylinders, these corrections are small in modulus with respect to unity: $b_{l,0}$ and $\langle b_{l,0} \rangle$ are close to S , and $|\delta_j| \ll S$. Noting that

$$T_{l,j,0,0} = H_0^{(1)}(kr_l^j) \approx \frac{2i}{\pi} \log(kr_l^j) + \left[1 + \frac{2i}{\pi} (\gamma - \log 2) \right], \tag{65}$$

with $kr_l^j \ll 1$, and remembering that δ_j is a deviation from a mean value, less than S in modulus, we see that

$$|D_1| \ll |D_2|.$$

Finally, neglecting D_1 in Eq. (64) yields

$$\langle b_{l,0} \rangle = \frac{S}{1 - \frac{S}{N} \sum_{l=1,N} \sum_{j \neq l} T_{l,j,0,0}}.$$

With the approximation of $T_{l,j,0,0}$ provided by relation (65), we get

$$\frac{1}{N} \sum_l \sum_{j \neq l} T_{l,j,0,0} = (N-1) \left[1 + \frac{2i}{\pi} (\gamma - \log 2) + \frac{2i}{\pi} \log(k\mathcal{L}) \right], \tag{66}$$

where

$$\mathcal{L} = \left(\prod_i \prod_{j \neq i} r_i^j \right)^{1/N(N-1)}. \tag{67}$$

Thus the value of $b_0 = N \langle b_{l,0} \rangle$ can be written as

$$b_0 = 1 / \left\{ -1 + \frac{1}{SN} + \frac{1}{N} - \frac{2i}{\pi} \frac{(N-1)}{N} \times \left[\gamma + \log\left(\frac{k\mathcal{L}}{2}\right) \right] \right\} = \frac{1}{-1 + iX}, \tag{68}$$

where the value of $S_{l,0,0} = S$ can be deduced from Eqs. (60) and (62):

$$\frac{1}{S} = -1 + i \left[\frac{-4}{\pi(\epsilon-1)(k\rho)^2} - \frac{2}{\pi} \log(k\rho) + \frac{1-4\gamma+4\log 2}{2\pi} - \frac{1}{\pi(\epsilon-1)} \right], \tag{69}$$

which finally gives the value of X in Eq. (68):

$$X = \frac{1}{N\pi} \left[\frac{-4}{(\epsilon-1)(k\rho)^2} - 2 \log(k\rho) + \frac{1-4\gamma+4\log 2}{2} - \frac{1}{(\epsilon-1)} \right] - \frac{2(N-1)}{N\pi} \left[\gamma + \log\left(\frac{k\mathcal{L}}{2}\right) \right].$$

The equivalence with a homogeneous cylinder is obtained by equalization of the values of X and \tilde{X} in Eqs. (60) and (68) and yields

$$\frac{1}{\tilde{\epsilon}-1} \left[\frac{1}{4} + \frac{1}{(k\tilde{R})^2} \right] = \frac{1}{N(\epsilon-1)} \left[\frac{1}{4} + \frac{1}{(k\rho)^2} \right] + \frac{1}{2} \log \left[\frac{(k\rho)^{1/N} (k\mathcal{L}/2)^{1-1/N}}{k\tilde{R}} \right] + \frac{1+4\log 2}{8} \left(1 - \frac{1}{N} \right). \tag{70}$$

Since $k\tilde{R}$ and $k\rho$ are small, the term $1/4$ is negligible compared with $1/(k\tilde{R})^2$ and $1/(k\rho)^2$. Thus Eq. (70) becomes

$$\tilde{\epsilon}-1 = (\epsilon-1) \frac{N\rho^2}{\tilde{R}^2} \frac{1}{1 + \frac{(\epsilon-1)N(k\rho)^2}{2}} \times \left[\log\left(\frac{\rho^{1/N} \mathcal{L}^{1-1/N}}{\tilde{R}}\right) + \frac{1}{4} \left(1 - \frac{1}{N} \right) \right]. \tag{71}$$

Remark: We can verify that this result agrees with the results obtained in Subsection 4.B. Indeed, when k tends to zero, Eq. (71) becomes

$$\tilde{\epsilon}-1 = (\epsilon-1)N\rho^2/\tilde{R}^2, \tag{72}$$

and the field diffracted by the set of cylinders is identical to $\tilde{b}_0 H_0^{(1)}(kr)$, with

$$\tilde{b}_0 = \frac{1}{-1 + i\tilde{X}} \approx \frac{1}{-1 + i[-4/\pi(\tilde{\epsilon}-1)(k\tilde{R})^2]} \approx \frac{i(\tilde{\epsilon}-1)k^2\pi\tilde{R}^2}{4} \approx \frac{i(\epsilon-1)k^2N\pi\rho^2}{4}. \tag{73}$$

One can also obtain this result by using Eq. (37), replacing $H_0^{(1)}(kPM)$ with $H_0^{(1)}(kr)$ and the total field $E(M)$ with its approximate value, which is none other than the incident field and consequently is equal to unity since the set of cylinders is located near the origin.

Let us come back to Eq. (71) and call a set of random cylinders one realization. A tedious and long calculation shows that the mean value of \mathcal{L} over a great number of realizations is equal to $R \exp(-1/4)$. In these conditions Eq. (71) simplifies to

$$\tilde{\epsilon}-1 = (\epsilon-1)(N\rho^2/\tilde{R}^2)1/(1+C), \tag{74}$$

with

$$C = \frac{(\epsilon-1)N(k\rho)^2}{2} \log\left(\frac{\rho^{1/N} R^{1-1/N}}{R}\right). \tag{74'}$$

Equation (74) gives the permittivity $\tilde{\epsilon}$ of the equivalent cylinder as a function of its radius \tilde{R} as soon as the parameters (N, ρ, ϵ, R) of the set of cylinders are known. For a given wavelength this relation shows that there exists an infinity of homogeneous cylinders ($\tilde{R}, \tilde{\epsilon}$) that are equivalent to the initial set of cylinders. There exists a value of \tilde{R} that is particularly interesting. Indeed, in the case for which

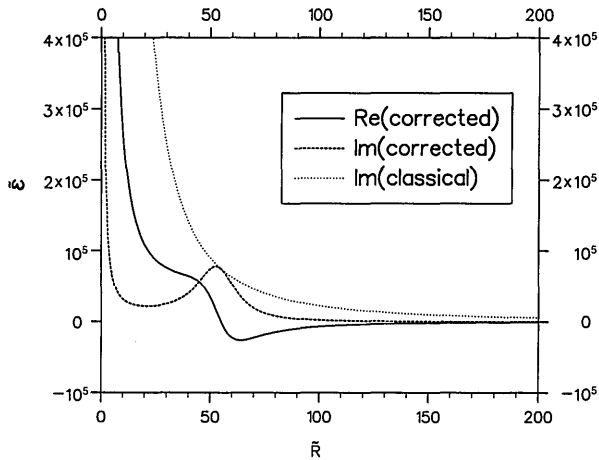


Fig. 14. Homogenization of a set of five cylinders.

$$\tilde{R} = R_0 = \rho^{1/N} R^{1-1/N}, \tag{75}$$

Eq. (74) becomes

$$\tilde{\epsilon} - 1 = (\epsilon - 1)(N\rho^2/\tilde{R}^2). \tag{76}$$

Equation (76) is none other than the relation given by the classical rule of homogenization, but it must be emphasized that now the radius of the homogeneous cylinder is given by Eq. (75) and thus differs from the actual radius R of the set of cylinders.

In order to estimate the influence of the corrective term C , let us consider the case of $N = 5$ circular cylinders of radius $\rho = 5 \mu\text{m}$ and conductivity $\sigma = 10^6 \Omega^{-1} \text{m}^{-1}$, randomly distributed in a circular domain of radius $R = 100 \mu\text{m}$, for a wavelength $\lambda = 30 \text{mm}$ and s polarization. In Fig. 14 we have plotted the characteristics of the homogeneous cylinder equivalent to this set of five cylinders, i.e., $\tilde{\epsilon}$ versus \tilde{R} , using successively Eqs. (74) (corrected permittivity) and Eq. (76) (classical permittivity). For these values the corrected permittivity is a complex number, whereas the classical permittivity is a purely imaginary number. Of course, the two equations give the same permittivity for the particular value $\tilde{R} = R_0 = 54.90 \mu\text{m}$. But it can be noted that for different values of the equivalent radius the curves differ significantly. In particular, a naive use of the classical rules of homogenization gives for an equivalent radius of $100 \mu\text{m}$ a permittivity $\tilde{\epsilon} = i22,500$, whereas the corrected value is $\tilde{\epsilon} = -6800 + i2300$. From the preceding results we can conclude that

1. The homogenization process does not satisfy the classical law.
2. In the infinite set of solutions $(\tilde{\epsilon}, \tilde{R})$ there exists one solution with a permittivity given by the classical rules of homogenization:

$$(\tilde{\epsilon} - 1)\tilde{R}^2 = (\epsilon - 1)N\rho^2,$$

but the radius R_0 of the equivalent homogeneous cylinder is less than the radius R of the domain containing the initial set of cylinders. The corrective term C of Eqs. (74) likely reflects the influence of boundary effects (the cylinders of C close to the boundary do not behave like the

other ones). Of course, it can be noticed that, when the density of the cylinders increases (i.e., N increases), the value of R_0 tends toward R , which agrees with the classical rule.

The particular value $\tilde{R} = R_0$ has interesting properties. When the cylinders are made with ohmic materials described by a conductivity σ and a permittivity $\epsilon = 1 + i\sigma/\epsilon_0\omega$, Eqs. (74) show that the permittivity $\tilde{\epsilon}$ of the homogeneous equivalent cylinder has a frequency behavior that differs from that of an ohmic material because of the presence of k in the correction C . On the other hand, if we choose the homogeneous equivalent cylinder with radius R_0 , the equivalent cylinder behaves as an ohmic material because Eq. (76) reduces to

$$\tilde{\sigma} = \sigma(N\rho^2/\tilde{R}^2), \tag{77}$$

where $\tilde{\sigma}$ is linked to $\tilde{\epsilon}$ by

$$\tilde{\epsilon} = 1 + i\tilde{\sigma}/\epsilon_0\omega. \tag{78}$$

In other words, it is only for this particular value R_0 that we can replace the set of ohmic cylinders by a homogeneous *ohmic* cylinder with a conductivity given by Eq. (77), thus *independent of the frequency* (as long as we stay in the low-frequency domain). This result can be helpful for the study of such set of cylinders in a given bandwidth.

Finally, let us compare these theoretical predictions with the rigorous numerical results provided by our computer code.

Figure 15 shows the scattered intensity generated by two sets of five cylinders, each of these sets being identical to the set of Fig. 14. The distance between the centers of the sets is equal to one wavelength, i.e., 30mm . The calculation was achieved on a single realization of the structure. The solid curve was computed with the actual set of ten elementary cylinders, and the dashed curve was computed by replacement of each group of five cylinders with the special homogeneous equivalent rod whose parameters are given by Fig. 14: $\tilde{R} = R_0 = \rho^{1/N} R^{1-1/N} = 54.90 \mu\text{m}$ and $\tilde{\epsilon} = i74,500$. The dotted curve gives the

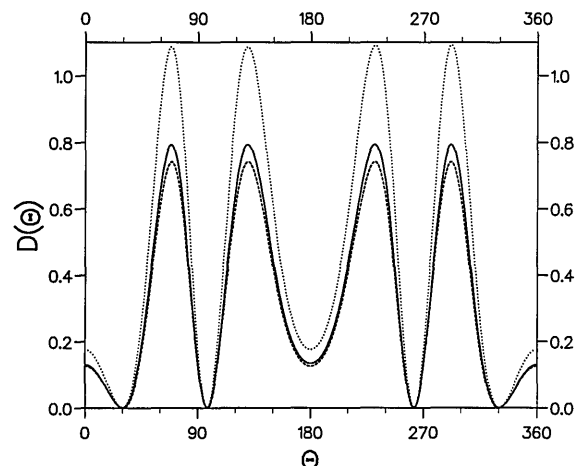


Fig. 15. Homogenization of two sets of five cylinders. Curves are defined in text.

intensity obtained by use of the classical rules of homogenization [i.e., with $\bar{\epsilon}$ given by Eq. (72) and the same radius $\bar{R} = R = 100 \mu\text{m}$]. It was verified that one obtains a much better agreement between the solid and the dashed curves by averaging the scattered intensity (solid curve) over many realizations.

6. CONCLUSION

A rigorous theory of scattering by N arbitrary-shaped cylinders arbitrarily located in space has been described and numerically implemented. Once the \mathbf{S} matrix of each cylinder is calculated precisely, this theory is able to provide, by inversion of a linear system, with good precision the intensity scattered by the set of cylinders. In the low-frequency domain, considerable simplification occurs, and the size of the linear system is drastically reduced.

The theory is especially suitable for the study of the phenomenon of enhanced backscattering by a set of arbitrary-shaped random rods. We were able to show that this phenomenon holds for p polarization when the index of the cylinders is low, in contrast to conjectures of other authors. For low frequencies the computation may be achieved for a large number of cylinders. In this domain it has been shown that the classical rules of homogenization should be corrected in some cases, and the corrections have been given.

Many other domains of investigation are currently being studied, in particular for random structures. For instance, studies of Anderson's localization of light by a set of random cylinders are in progress.

REFERENCES

1. D. Maystre and J. C. Dainty, *Modern Analysis of Scattering Phenomena* (Hilger, Bristol, UK, 1992).
2. M. Abramovitz and I. Stegun, *Handbook of Mathematical Functions* (Dover, New York, 1970).
3. J. Y. Suratteau and R. Petit, "The electromagnetic theory of the infinitely conducting wire grating using a Fourier-Bessel expansion of the field," *Int. J. Infrared Millimeter Waves* **5**, 1189-1200 (1984).
4. R. C. McPhedran, "Transport properties of cylinder pairs and of the square array of cylinders," *Proc. R. Soc. London Ser. A* **408**, 31-43 (1986).
5. R. C. McPhedran, L. Poladian, and G. W. Milton, "Asymptotic studies of closely spaced, highly conducting cylinders," *Proc. R. Soc. London Ser. A* **415**, 185-196 (1988).
6. H. A. Youssif and S. Köhler, "Scattering by two penetrable cylinders at oblique incidence. I. The analytical solution," *J. Opt. Soc. Am. A* **5**, 1085-1096 (1988).
7. A. Z. Elsherbeni and A. A. Kishk, "Modeling of cylindrical objects by circular dielectric and conducting cylinders," *IEEE Trans. Antennas Propag.* **40**, 96-99 (1992).
8. J. Van Bladel, *Electromagnetic Fields* (McGraw-Hill, New York, 1964).
9. L. Schwartz, *Mathematics for Physical Sciences* (Addison-Wesley, London, 1967).
10. D. Maystre and P. Vincent, "Diffraction d'une onde électromagnétique plane par un objet cylindrique non infiniement conducteur de section arbitraire," *Opt. Commun.* **5**, 327-330 (1972).
11. F. Zolla, R. Petit, and M. Cadilhac, "Electromagnetic theory of diffraction by a system of parallel rods: the method of fictitious sources," *J. Opt. Soc. Am. A* **11**, 1087-1096 (1994).
12. K. A. O'Donnell and E. R. Mendez, "Experimental study of scattering from characterized random surfaces," *J. Opt. Soc. Am. A* **4**, 1194-1205 (1987).
13. M. Nieto-Vesperinas and J. M. Soto-Crespo, "Monte Carlo simulations for scattering of electromagnetic waves from perfectly conductive random rough surfaces," *Opt. Lett.* **12**, 979-981 (1987).
14. J. M. Soto-Crespo and M. Nieto-Vesperinas, "Electromagnetic scattering from very rough random surfaces and deep reflection gratings," *J. Opt. Soc. Am. A* **6**, 367-384 (1989).
15. A. R. McGurn, A. A. Maradudin, and V. Celli, "Localization effects in the scattering of light from a randomly rough grating," *Phys. Rev. B* **31**, 4866-4871 (1985).
16. A. A. Maradudin, E. R. Mendez, and T. Michel, "Backscattering effects in the elastic scattering of p -polarized light from a large-amplitude random metallic grating," *Opt. Lett.* **14**, 151-153 (1989).
17. M. Saillard and D. Maystre, "Scattering from metallic and dielectric rough surfaces," *J. Opt. Soc. Am. A* **7**, 982-990 (1990).
18. J. J. Greffet, "Backscattering of s -polarized light from a cloud of small particles above a dielectric substrate," *Waves Random Media* **3**, S65-S73 (1991).